



OPEN

DATA DESCRIPTOR

# Multi-model hydrological reference dataset over continental Europe and an African basin

Bram Droppers<sup>1</sup>✉, Oldrich Rakovec<sup>2,3</sup>✉, Leandro Avila<sup>4</sup>, Shima Azimi<sup>5</sup>, Nicolás Cortés-Torres<sup>6</sup>, David De León Pérez<sup>6,7</sup>, Ruben Imhoff<sup>8</sup>, Félix Francés<sup>6</sup>, Stefan Kollet<sup>4</sup>, Riccardo Rigon<sup>5</sup>, Albrecht Weerts<sup>8,9</sup> & Luis Samaniego<sup>2,10</sup>

Although Essential Climate Variables (ECVs) have been widely adopted as important metrics for guiding scientific and policy decisions, the Earth Observation (EO) and Land Surface and Hydrologic Model (LSM/HM) communities have yet to treat terrestrial ECVs in an integrated manner. To develop consistent terrestrial ECVs at regional and continental scales, greater collaboration between EO and LSM/HM communities is needed. An essential first step is assessing the LSM/HM simulation uncertainty. To that end, we introduce a new hydrological reference dataset that comprises a range of 19 existing LSM/HM simulations that represent the current state-of-the-art of our LSM/HMs. Simulations are provided on a daily time step, covering Europe, notably the Rhine and Po river basins, alongside the Tugela river basin in Africa, and are uniformly formatted to allow comparisons across simulations. Furthermore, simulations are comprehensively validated with discharge, evapotranspiration, soil moisture and total water storage anomaly observations. Our dataset provides valuable information to support policy development and serves as a benchmark for generating consistent terrestrial ECVs through the integration of EO products.

## Background & Summary

Essential Climate Variables (ECVs) are a group of bio-physical variables that are critical for understanding and characterizing Earth's climate<sup>1</sup>. Therefore, this relatively limited set of variables are vital “to guide mitigation and adaptation measures, to assess risks and enable attribution of climate events to underlying causes, and to underpin climate services”<sup>2</sup>. Originally conceptualized by the Global Climate Observing System (GCOS) in the 1990s, the ECVs framework has gained widespread adoption in scientific and policy domains. Various climate agencies and organizations, including the United Nations Framework Convention on Climate Change (UNFCCC), the World Meteorological Organization (WMO) and the Intergovernmental Panel on Climate Change (IPCC), rely on ECVs as guiding metrics. GCOS currently identifies 55 ECVs, classifying them into three main categories: atmospheric, terrestrial and oceanic variables<sup>3</sup>.

In order to evaluate large-scale climatic patterns, a consistent, extensive and continuous estimation of ECVs is needed. Such estimations can be achieved by merging observations, that are limited in time and space, with computational models, that can consistently fill the gaps between observations. Although various reanalysis

<sup>1</sup>Department of Physical Geography, Utrecht University, P.O. Box 80.115, 3508 TC, Utrecht, The Netherlands.

<sup>2</sup>Department of Computational Hydrosystems, UFZ-Helmholtz Centre for Environmental Research, Permoserstraße 15, 04318, Leipzig, Germany. <sup>3</sup>Faculty of Environmental Sciences, Czech University of Life Sciences Prague, Praha-Suchbát, 16500, Czech Republic. <sup>4</sup>Institute of Bio- and Geosciences Agrosphere (IBG-3), Research Centre Jülich, Wilhelm-Johnen-Straße, 52428, Jülich, Germany. <sup>5</sup>Center Agriculture, Food and Environment (C3A), Department of Civil, Environmental and Mechanical Engineering, University of Trento, via Mesiano 77, 38123, Trento, Italy. <sup>6</sup>Research Group of Hydrological and Environmental Modelling (GIMHA), Research Institute of Water and Environmental Engineering (IIAMA), Universitat Politècnica de València, Cami de Vera S/N, 46022, Valencia, Spain. <sup>7</sup>GeoAgro-Environmental Sciences and Resources Research Center Foundation (CENIGAA), 8th-Str. 32-49, 410001, Neiva, Huila, Colombia. <sup>8</sup>Operational Water Management & Early Warning Department, Deltares, P.O. Box 177, 2600 MH, Delft, The Netherlands. <sup>9</sup>Hydrology and Environmental Hydraulics group, Wageningen University and Research, P.O. Box 47, 6700 AA, Wageningen, The Netherlands. <sup>10</sup>Institute of Environmental Science and Geography, University of Potsdam, Karl-Liebknecht-Str. 24-25, 14476, Potsdam, Germany. ✉e-mail: [b.droppers@uu.nl](mailto:b.droppers@uu.nl); [oldrich.rakovec@ufz.de](mailto:oldrich.rakovec@ufz.de)

products estimate atmospheric and oceanic ECVs<sup>4,5</sup>, important terrestrial ECVs such as the terrestrial water cycle components<sup>6</sup> have yet to be treated in an integrated manner by the Earth Observation (EO) water cycle community and Land Surface and Hydrologic Model (LSM/HM) communities<sup>7</sup>. For instance, in estimating evapotranspiration, Surface Vegetation-Atmosphere Transfer (SVAT) schemes do not necessarily close the water balance in gauged basins<sup>8</sup>. Likewise, in reconstructing streamflow at a regional or continental scale, little or no input from EO systems is generally used<sup>9–11</sup>. Consequently, the EO and LSM/HM communities have yet to treat the water cycle as a unique system consistently.

To advance the generation of high-resolution terrestrial ECVs, the European Space Agency (ESA) initiated the “*Hyper-resolution Earth observations and land-surface modeling for a better understanding of the water cycle*” project, referred to as 4DHydro (4D refers to time and space). This initiative aims to facilitate extensive collaboration between the EO and LSM/HM communities, striving for better integration between innovative high-resolution satellite products and hyper-resolution modeling of the hydrological cycle. For example, from an EO perspective, the project will explore the potential benefits of LSM/HM simulations in enhancing the down-scaling of satellite products and achieving water balance closure. In contrast, from an LSM/HM perspective, the project will explore the added value of assimilating EO products, through data assimilation and calibration, on high-resolution hydrological simulations. An essential first step of 4DHydro, presented here, involves a comprehensive assessment of the uncertainty inherent in existing LSM/HM datasets concerning key hydrological variables. Such an assessment will give a better understanding of the limitations in generating high-resolution terrestrial ECVs and will be used as a baseline for LSM/HM performance under EO integration. To that end, we introduce a new hydrological reference dataset.

Our hydrological reference dataset comprises 19 existing LSM/HM simulations from previous studies and represents the current state-of-the-art of our LSM/HMs. The dataset covers four study regions, namely continental Europe, the European Po and Rhine river basins and the Tugela river basin in Africa, and includes four hydrological variables on a daily time step, namely discharge, evapotranspiration, soil moisture content and total water storage (Data Records Section). Our dataset covers a diverse range of LSM/HM simulations with 8 different land-surface and hydrological models from the 4DHydro project and 7 different meteorological input datasets (Methods Section), thereby capturing both systemic and input uncertainties. Despite this diversity, simulations in our hydrological reference dataset are uniformly formatted following our storage protocol (see Data Records Section), which allows for seamless comparisons across simulations. Additionally, we present a performance benchmark of our LSM/HM simulations (Technical Validation Section). The benchmark comprehensively validates the simulations of our hydrological dataset using observations from discharge gauges (from GRDC, LamaH-CE, CAMELS-GB, CAMELS-CH and various local datasets), evapotranspiration towers (from FLUXNET), soil moisture stations (from ISMN) and total water storage anomaly satellite products (from GRACE and GRACE-FO).

LSM/HMs simulations of our hydrological reference dataset are publicly available through the open science catalog at [4dhydro.eu/catalog](https://4dhydro.eu/catalog) (Usage Notes section) to enable open collaboration with end-users, including the scientific community and the general public. Our hydrological reference dataset serves dual purposes: (1) the dataset provides valuable and publicly accessible information to support policy development in the regions of interest and (2) the dataset functions as a benchmark for generating high-resolution terrestrial ECVs, through the integration of EO products, during subsequent stages of the 4DHydro initiative. In these next stages, LSM/HM simulations will be improved through calibration, assimilation and validation with high-resolution EO products. These improved simulations, and the high-resolution EO products, will also be made available through the open science catalog. Considering that the main aim of the 4DHydro initiative is to facilitate collaboration, we welcome the scientific community to contribute to our hydrological reference dataset following the approach outlined here.

## Methods

The 19 simulations in the reference dataset are derived from combinations of eight existing Land-Surface Model and Hydrological Models (LSM/HMs) and seven meteorological datasets. This section provides a concise description of the LSM/HMs, their main references and parameterization, and the meteorological datasets.

**Land-Surface and Hydrological Models (LSM/HMs).** The reference dataset includes eight LSM/HMs: Community Land Model (CLM), GEOframe, mesoscale Hydrologic Model (mHM), Parflow-CLM, PCRaster Global Balance (PCR-GLOBWB), TETIS, Terrestrial Systems Modeling Platform (TSMP) and `wflow_sbm`. Table 1 presents the used data sets for the model parameterization.

These models represent a diverse range of model structures, conceptualizations and implementations. For example, most models are distributed models, which simulate hydrology on a grid, except for the GEOframe model which is a semi-distributed model that simulates hydrology per sub-basin. Additionally, components such as lateral groundwater flows are implemented in Parflow-CLM, TSMP and `wflow_sbm`, whereas human impacts are implemented in PCR-GLOBWB (water use and reservoir operations) and `wflow_sbm` (reservoir operations). Lastly, several models rely on calibration, either directly (GEOframe and TETIS) or through transfer functions (mHM), whereas the other models only spin-up their initial conditions. Although all these model differences carry their benefits and uncertainties, all models are included in our reference dataset to capture both systemic and input uncertainties.

**Community Land Model (CLM).** CLM simulates land surface processes in global climate studies as part of the Community Climate System Model (CCSM3)<sup>12–14</sup>. These processes encompass biophysics, radiation interactions, heat transfer, hydrology and vegetation characteristics. The model accounts for plant functional types and soil properties<sup>15</sup>. CLM version 3.5, the version used here, introduces significant changes in its hydrological

Model	Landsurface	Landcover	Hydrogeology	Water use	Glaciers
CLM	DSMW <sup>136</sup>	MODIS LC <sup>137</sup>	—	—	—
GEOframe	Regional DEM	—	—	—	—
mHM	SoilGrids <sup>138</sup> , GMTED 2010 <sup>139</sup> , HydroSHEDS <sup>140</sup>	GLOBCOVER <sup>141</sup> , GIMMS MODIS <sup>142</sup>	GLIM <sup>143</sup>	—	—
Parflow-CLM	SoilGrids250m <sup>138</sup> , USDA <sup>144</sup>	CLC 2018 <sup>145</sup>	IHME1500 <sup>146</sup>	—	—
PCR-GLOBWB	DSMW <sup>136</sup> , HydroSHEDS <sup>140</sup> , GTOPO30 <sup>147</sup> , Hydro1k <sup>148</sup>	GLCC <sup>149</sup> , MIRCA2000 <sup>152</sup>	GLHYMPS <sup>150</sup>	GLWD <sup>151</sup> , GRanD <sup>153</sup>	—
TETIS	SoilGrids <sup>138</sup> , GMTED2010 <sup>139</sup> , HydroSHEDS <sup>140</sup>	GLOBCOVER <sup>141</sup> , GIMMS MODIS <sup>142</sup>	GLIM <sup>143</sup>	—	—
TSMP	SMW <sup>154</sup> , GTOPO30 <sup>147</sup>	GLOBCOVER <sup>141</sup> , ODIS LC <sup>137</sup>	—	—	—
wflow_sbm	SoilGrids <sup>138</sup> , MERIT Hydro DEM <sup>155</sup>	VITO v2 <sup>156</sup> , CLC 2018 <sup>145</sup> , MODIS LAI <sup>157</sup>	—	HydroLAKES <sup>158</sup> , GRanD <sup>153</sup>	Global RGI <sup>159</sup> , GLIMS <sup>160</sup> , GLAMOS <sup>161</sup>

**Table 1.** Summary of data sources used as input for each land surface and hydrological model.

cycle simulation. These include updated surface datasets<sup>16</sup>, an improved canopy integration scheme<sup>17</sup>, scaled canopy interception<sup>18</sup>, a simplified TOPMODEL-based runoff model<sup>19</sup>, a groundwater model that considers water exchange in the vertical direction<sup>20</sup> and a new frozen soil scheme<sup>21</sup>. CLM has been used to simulate and assimilate tECVs in various regions such as Europe<sup>22</sup> and China<sup>23</sup>. Although later versions of CLM (4.0 and 4.5) exhibit a better parametrization, previous studies indicate that the differences between CLM3.5 and later versions are small when comparing soil moisture variability to observations<sup>24</sup>. For the CLM simulations in the reference dataset, no calibration was required. Instead, CLM considers a spin-up of initial conditions and states up to a dynamic equilibrium.

**GEOframe.** GEOframe is a versatile computer-based hydrology system. GEOframe offers diverse modeling solutions with components built on the Object Modeling system framework<sup>25</sup>, which accommodates various modeling paradigms, including process-based<sup>26</sup>, lumped<sup>27</sup> and machine learning<sup>28</sup> paradigms. These components cover rainfall-runoff<sup>29</sup>, snow<sup>30</sup>, evaporation, transpiration<sup>31</sup>, infiltration<sup>26</sup>, terrain analysis<sup>32</sup>, interpolation<sup>33</sup>, calibration<sup>25</sup> and more. The system is designed for adaptability and stability and handles spatially disjoint catchments. GEOframe has been used to simulate tECVs at different scales from point to large catchments<sup>34</sup> and in various regions<sup>35</sup>. For the GEOframe simulations in the reference dataset, all crucial process-based modules necessary for geomorphological analysis, water budget calculation (i.e. canopy, snow, soil moisture and groundwater) and river discharge routing are included. Furthermore, 18 parameters were optimized (in terms of Kling-Gupta Efficiency) using the calibration process of the GEOframe system framework<sup>36</sup>.

**mesoscale Hydrologic Model (mHM).** mHM is a gridded distributed hydrological model developed by Helmholtz Centre for Environmental Research GmbH (UFZ)<sup>37–40</sup>. The model covers processes like canopy interception, snow accumulation and melt, soil moisture dynamics, infiltration, surface runoff, evapotranspiration, deep percolation, subsurface storage, baseflow, discharge generation, discharge attenuation and flood routing. The model source code is highly modular and is written in Fortran. A particular feature of mHM is the original implementation of the multiscale parameter regionalization scheme. This scheme allows model parameters to be transferred across scales and locations with great computational efficiency and a minimum decrement in performance<sup>41</sup>. mHM has been used to simulate tECVs in over 1 000 European basins and globally over 5 000+ GRDC basins of varying sizes and diverse spatial resolutions (from 1 by 1 km to 100 by 100 km)<sup>42–46</sup> and is currently operational in the ULYSSES C3S global seasonal forecasting system and in the German Drought Monitor<sup>47</sup>. For the mHM simulations in the reference dataset, two different global parameter sets were used in this study: the default parameterization for the Rhine, Po and Tugela river basins<sup>48</sup> and a compromise solution, constrained over six randomly selected European basins, for continental Europe. This random selection of six basins was repeated a hundred times. Then, the best-performing parameter cross-evaluated over 958 European basins (in terms of the median Kling-Gupta Efficiency) was selected<sup>49</sup>.

**Parflow-CLM.** Parflow is an integrated subsurface and surface hydrological model that simulates 3D variably saturated groundwater flow using the Richards equation and incorporates a 2D overland flow as a free surface boundary condition<sup>50,51</sup>. As the standalone ParFlow cannot account for land surface processes (e.g., evapotranspiration and snow water equivalent), this model is generally coupled to the Common Land Model (CLM), which is a modified version of the original Common Land Model<sup>52</sup>. Note that the Common Land Model (CLM) is not the same land surface model as the community land model (see CLM section), which is the land component of the Community Earth System Model (CESM). CLM provides the sources and sinks for soil moisture to Parflow whereas, to calculate the land surface water and energy balances, CLM receives from ParFlow spatially distributed soil moisture and soil matric potential. Parflow-CLM has been applied to simulate tECVs from test sites to the continental scale, from sub-daily to climate time scales, and range from scientific research to quasi-operational use around the world<sup>50,53–55</sup>. The Parflow-CLM simulations in the reference dataset include

the so-called DE06<sup>55</sup> domain which extends over the Rhine basin. Here, the model considers a spin-up of initial conditions and states up to a dynamic equilibrium, so no calibration is required.

**PCRaster Global Water Balance (PCR-GLOBWB).** PCR-GLOBWB is a grid-based global hydrology and water resources model developed at the Department of Physical Geography, Faculty of Geosciences, Utrecht University, the Netherlands<sup>56,57</sup>. PCR-GLOBWB describes the terrestrial part of the hydrological cycle. For each grid cell and each day, PCR-GLOBWB simulates moisture storage as well as the water exchange between the soil, atmosphere and underlying groundwater reservoir. River discharge is calculated by accumulating and routing specific runoff along the drainage network. A particular feature of PCR-GLOBWB is that human water use is fully integrated with the hydrological cycle. Livestock, industry and households water demands are estimated based on socio-economic developments whereas irrigation water demands are dynamically calculated. These demands are subsequently translated into actual withdrawals from groundwater and surface water (rivers, lakes and reservoirs) subject to water availability and the maximum groundwater pumping capacity<sup>58</sup>. Since the model was first introduced, PCR-GLOBWB has been applied extensively to simulate tECVs in global water resource assessments ranging from 30 arc-minutes (50 by 50 km at the equator) to 30 arc-seconds (1 by 1 km at the equator) spatial resolutions<sup>59–67</sup>. For the PCR-GLOBWB simulations in the reference dataset, the default model parameterization<sup>57</sup> without any calibration is used.

**TETIS.** TETIS is a spatially distributed eco-hydrological model<sup>68,69</sup>, that has been under development by the Instituto de Ingeniería del Agua y Medio Ambiente (IIAMA) of Universitat Politècnica de València (UPV) since 1995. The model accommodates various spatial scales, from under 1 km<sup>2</sup> to 60 000 km<sup>2</sup>, spatial resolutions and multiple climatic conditions worldwide. TETIS accounts for spatial heterogeneity in its inputs, parameters and state variables and offers sub-modules such as reservoir operation, snow accumulation and melting, sediment erosion, transport and deposition, nitrogen cycle, natural dynamic vegetation, flood and drip irrigation and crop production<sup>70–74</sup>. This version of TETIS employs the traditional vertical conceptualization first introduced in Tetis V9.1, which is concerned with the vertical movement of water between different tanks. Additionally, it incorporates the horizontal structure regarding the movement of water across the drainage network, as derived from the mHM model. TETIS has been employed to evaluation Sentinel-1, SMAP and SMOS surface soil moisture products for distributed eco-hydrological modeling<sup>75,76</sup>. For the TETIS simulations on the reference data set, the default geologic units of mHM were employed. The nine corrector factors of the Tetis model were calibrated against daily observed data from discharge gauges using the Shuffled Complex Evolution (SCE) algorithm to optimize the Kling-Gupta Efficiency.

**Terrestrial Systems Modeling Platform (TSMP).** TSMP is a fully coupled terrestrial model closing the water and energy balance from groundwater across the land surface to the top of the atmosphere<sup>77,78</sup>. TSMP integrates Parflow-CLM (see Parflow-CLM subsection) to represent the land-surface and the Consortium for Small-scale Modeling (COSMO)<sup>79</sup>, the former weather prediction system of the German Weather Service, to represent atmospheric processes. The land-surface and atmospheric models are coupled via the external coupler OASIS3-MCT<sup>80</sup>, allowing TSMP to run in fully coupled mode (COSMO - ParFlow-CLM), where the lower boundary information for COSMO is provided by ParFlow-CLM. For more details, including the implementation over the European CORDEX domain, the reader is referred to Furusho-Percot *et al.*<sup>81</sup>. TSMP has been used to simulate fully coupled tECVs in Europe<sup>82,83</sup>. For the TSMP simulations in the reference dataset, no calibration was required. Instead, TSMP considers a spin-up of initial conditions and states up to a dynamic equilibrium.

**wflow\_sbm.** wflow\_sbm is an open-source distributed hydrological model developed by Deltares and written in Julia<sup>84</sup>. The soil setup of the model was originally based on the topog\_sbm (soil bucket model) concept<sup>85</sup>. Wflow\_sbm tries to balance low-resolution, low-complexity (conceptual) and high-resolution, high-complexity (physics-based) hydrological models. This is attained by having parameters based on physical characteristics or processes while keeping relatively fast run times. The wflow\_sbm model includes hydrological processes such as glacier and snow processes, lakes and reservoirs (and their operations), evapotranspiration processes, unsaturated zone dynamics, lateral subsurface flow processes and multiple surface flow routing modules. Wflow\_sbm models can be easily derived and parameterized for any catchment with the Python tool HydroMT-Wflow<sup>86</sup>. This tool uses globally available datasets and derives the river morphology (river network, flow directions, river width, etc.)<sup>87</sup> and subsequently derives parameter values through the use of (pedo)transfer functions and suitable upscaling rules<sup>88</sup>. wflow\_sbm has been applied to simulate tECVs around the world at various spatial resolutions<sup>89–92</sup>. For the wflow\_sbm simulations in the reference dataset, the default parameter derivation has been applied without any further calibration.

**Meteorological Datasets.** The land-surface and hydrological models described above are forced, in total, with seven meteorological datasets, namely the E-OBS, EMO-1, ERA-5, ERA-I, HRES, COSMO-REA6 and measurement datasets. All models except for CLM, ParFlow-CLM and TSMP require precipitation, temperature and potential evapotranspiration to run. Potential evapotranspiration is calculated using Priestley Taylor<sup>93</sup> for GEOframe, Hargreaves Samani<sup>94</sup> for mHM and TETIS, Penman-Monteith<sup>95</sup> for PCR-GLOBWB and de Bruin<sup>96</sup> for wflow\_sbm. CLM, ParFlow-CLM and TSMP additionally require relative humidity, wind speed, surface pressure and surface radiation. TSMP uses these variables only as a boundary condition and dynamically simulates meteorology (see TSMP section).

**E-OBS<sup>97,98</sup>** is a gridded ensemble dataset based on the interpolation of meteorological station observations from the European Climate Assessment & Dataset (ECA&D)<sup>99,100</sup>. The ensemble comes from stochastic simulations that produce an ensemble of realizations based on the residuals of the initial (deterministic) interpolation. E-OBS provides daily estimates of precipitation, temperature, sea level pressure, global radiation and wind speed



Model	Meteorology	Resolution	Period	Regions	Variables	References
CLM	CRA6	0.0275 degrees	'95-'18	Europe, Po and Rhine	et, q, sm, tws	<sup>162</sup>
GEOframe	measurements	30 arc-seconds (sub-basin)	'15-'18	(upper) Po	et, q, sm, tws	<sup>163</sup>
mHM	EMO-1	0.125 degrees	'90-'21	Po and Rhine	et, q, sm, tws	<sup>164</sup>
		0.015625 degrees	'90-'21	Po and Rhine	et, q, sm, tws	
	E-OBS	0.125 degrees	'90-'21	Europe, Po and Rhine	et, q, sm, tws	
	ERA-5	0.125 degrees	'90-'21	Europe, Po, Rhine and Tugela	et, q, sm, tws	
Parflow-CLM	HRES	0.0055 degrees	'13-'21	Rhine	et, q, sm, tws	<sup>162</sup>
PCR-GLOBWB	ERA-I	5 arc-minutes	'90-'15	Europe, Po, Rhine and Tugela	et, q, sm, tws	<sup>165</sup>
TETIS	ERA-5	0.0625 degrees	'90-'20	Po and Tugela	et, q, sm, tws	<sup>166,167</sup>
TSMP	ERA-I (dynamic)	0.11 degrees	'96-'17	Europe, Po and Rhine	et, q, sm, tws	<sup>162</sup>
wflow_sbm	ERA-5	30 arc-seconds	'90-'22	Po, Rhine and Tugela	et, q, sm	<sup>168</sup>
				Europe	q	

**Table 2.** Available simulations by model, meteorology, resolution, regions and variables. References to the simulation storage repositories are also included. Note that GEOframe operates on a sub-basin resolution, only in the upper Po region, but outputs are reported on a 30 arc-second grid. Also note that the TSMP simulations use ERA-I for the atmospheric boundary conditions but dynamically simulation the atmosphere using COMOS.

for Europe. Data is available from 1950s until near real-time, at two spatial resolutions (0.1 by 0.1 degrees and 0.25 by 0.25 degrees).

*European Meteorological Observations (EMO-1)* is a gridded ensemble dataset based on the interpolation of a historical and real-time meteorological observations from a range of data providers<sup>101</sup>. EMO-1 provides (sub-)daily estimates of precipitation, temperatures (minimum and maximum), wind speed, solar radiation and water vapour pressure for Europe. Data is available from 1990 until 2022 for the newest EMO version, at 1 by 1 arc-minutes spatial resolution (EMO-1), which replaces the previous version at 5 by 5km spatial resolution (EMO-5).

*ECMWF ReAnalysis 5 (ERA-5)*<sup>102</sup> is the latest generation of atmospheric reanalysis by the European Centre for Medium-Range Weather Forecasts (ECMWF). ERA-5 provides gridded hourly estimates of a wide range of meteorological variables throughout the atmosphere and at the land surface around the world. Data is available from 1940 until near real-time at 30 by 30km spatial resolution. ERA-5 replaces its predecessor *ECMWF ReAnalysis Interim (ERA-I)*<sup>103</sup> which provided the same variables from 1979 to 2019 at a 80 by 80km spatial resolution.

*ECMWF High Resolution (HRES)* is a deterministic medium-range forecast<sup>104</sup> based on the European Centre for Medium-Range Weather Forecasts (ECMWF) high-resolution atmospheric model. Each day, HRES offers a single gridded forecast that describes the evolution of the weather out to 10 days ahead at a spatial resolution of 0.1 by 0.1 degrees. Data is available from 2010-09 until near real-time.

*COSMO ReAnalysis 6 (COSMO-REA6)*<sup>105</sup>, is an atmospheric reanalysis using the Consortium for Small-scale Modeling (COSMO) model. COSMO-REA6 provides gridded hourly estimates of a wide range of meteorological variables throughout the atmosphere and at the land surface for Continental Europe. Data is available from 1995 until 2019 at 0.055 by 0.055 degrees spatial resolution.

*measurements* include ground-based daily precipitation and temperature observations over the Aosta Valley (the upper part of the Po River basin) for the period of 2005-2021<sup>106</sup>.

## Data Records

Our hydrological reference dataset consists of land-surface and hydrological simulations with various configurations (Table 2). Simulations are available in Network Common Data Form (NetCDF) files. Files are named following their respective simulation in the format: model, meteorological forcing, variable, region, spatial resolution, temporal resolution, start date and end date, all lowercase, separated by underscores ( \_ ) and appended by the NetCDF extension (.nc). For example: *pcrglobwb\_ERA-I\_et\_europe\_05min\_daily\_1990101\_19901231.nc*.

NetCDF files are consistently formatted following our storage protocol (see Supplementary Information). All latitudes and longitudes are reported using the World Geodetic System 84 (WGS 84) with the same bounds for each region. Most simulations start in the 1990s and end in the 2010s. Simulations are split into multiple yearly or monthly files to reduce the file size if necessary (e.g. for higher spatial resolutions). Four key hydrological variables are provided at a daily timestep, namely discharge ( $q$ ;  $m^3 s^{-1}$ ), evapotranspiration ( $et$ ;  $kg m^2 s^{-1}$ ), soil moisture content ( $sm$ ; % of soil volume) and total water storage ( $tws$ ;  $kg m^2$ ). Note that soil moisture can be reported for multiple soil layers with varying depths. Besides the hydrological variables, a catchment mask and upstream area are provided for each region to aid in the validation.

## Technical Validation

Although the LSM/HM conceptualization, implementation and setup differ substantially within our hydrological reference dataset, they aim to simulate the same hydrological processes. Moreover, simulations are uniformly formatted following our storage protocol (see Data Records Section). Therefore, a comprehensive validation is warranted.

**Validation Data.** To validate our hydrological reference dataset, simulations are compared with observed data collected from discharge gauges, evapotranspiration towers, soil moisture stations and total water

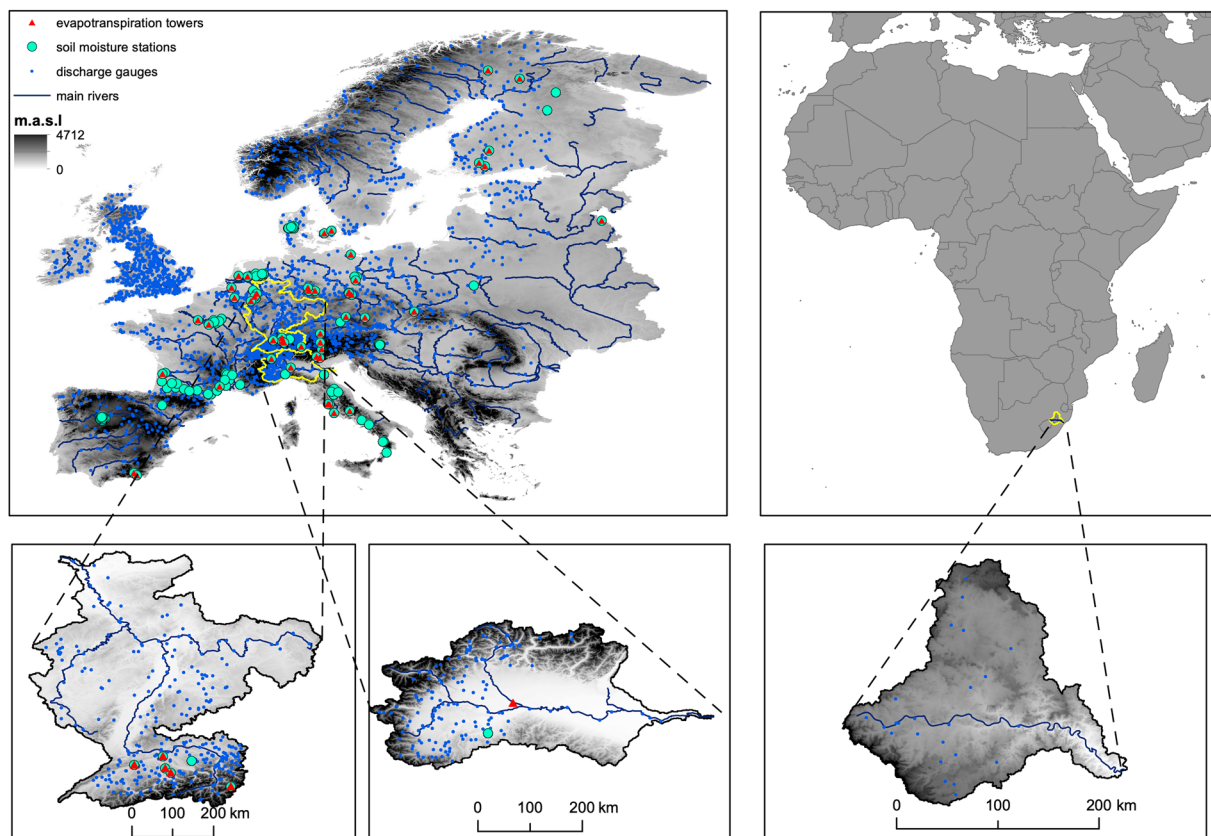


**Fig. 1** Discharge (blue), evapotranspiration (red) and soil moisture (cyan) observation locations for the four regions of interest: Europe, including the Rhine and Po basin, and the Tugela basin in Africa.

storage anomaly satellites (Fig. 1). Specifically, discharge data originate from the Global Runoff Data Centre dataset (GRDC)<sup>107</sup>, large-sample data for hydrology and environmental sciences in central Europe dataset (LamaH-CE)<sup>108</sup>, catchment attributes and meteorology for large-sample studies in Great Britain dataset (CAMELS-GB)<sup>109</sup>, catchment attributes and meteorology for large-sample studies in Switzerland dataset (CAMELS-CH)<sup>110</sup> and various local datasets<sup>106,111–114</sup>. Evapotranspiration data are obtained from the FLUXNET 2015 dataset (FLUXNET2015)<sup>115</sup>, while soil moisture observations are taken from the International Soil Moisture Network dataset (ISMN)<sup>116,117</sup>. Total water storage anomaly data originate from the Gravity Recovery and Climate Experiment (GRACE) and its follow-on satellite mission (GRACE-FO)<sup>118</sup>. Four GRACE solutions are included: the Jet Propulsion Laboratory (JPL) spherical<sup>119,120</sup> and mascon solution<sup>121</sup>, the University of Texas Center for Space Research (CSR) spherical solution<sup>122,123</sup> and the GeoForschungsZentrum (GFZ) spherical solution<sup>124,125</sup>.

**Validation Approach.** Evapotranspiration and soil moisture observations are compared directly to the simulated grid cell closest to the reported observation location. Note that these comparisons are inherently limited due to the nature of our data. Grid-cell outputs represent an average value across the entire grid cell, while point-observation outputs correspond to a specific location, in the case of soil moisture content, or a relatively small area in the case of evapotranspiration. Particularly important is that variations in soil parameters, such as soil porosity, between point observations and grid-cell averages can introduce significant biases in the simulated soil moisture content. Therefore, soil moisture observations are compared as anomalies by subtracting the mean over the comparison period.

A different approach was taken for the evaluation of the discharge observations. Rather than comparing discharge directly to the grid cell closest to the reported observation location, observations are matched to a neighbouring grid cell that best corresponds to the reported upstream area. The nearest grid cells within a quarter arc degree from the reported station location where the upstream area difference is smaller than a tenth (or the minimum) is selected. Some local discharge observation datasets did not provide information about the station's upstream area. In such cases, we used the reported average discharge difference for the selection.

Model evaluations of total water storage anomalies are spatially averaged per region, leading to a single time series per region. We used this approach because satellite-based terrestrial water storage anomaly signals undergo spatial smoothing and filtering. This process can result in signals from neighbouring areas affecting the observations, also known as “leakage”<sup>126</sup>. Spatial averaging of the observation-based products helps minimise the leakage signals’ influence.

**Simulation Selection.** For our comparison, we made a sub-selection of the available observation data, considering the common simulation period and the common simulation geographical domain of each region and

Variable	Common region	Common period	Observation number (#)	Observation average duration (years)
Discharge	Europe	'96-'15	2899	18.0
	Po basin	'96-'15	163	13.0
	Rhine basin	'96-'15	354	19.3
	Tugela basin	'90-'15	27	22.2
Evapotranspiration	Europe	'96-'15	56	10.0
	Po basin	'96-'15	1	3.0
	Rhine basin	'96-'15	6	11.2
Soil moisture content	Europe	'96-'15	252	5.6
	Po basin	'96-'15	8	3.5
	Rhine basin	'96-'15	1	4.6
Total water storage anomaly	Europe	'96-'15	4	12.3
	Po basin	'96-'15	4	12.3
	Rhine basin	'96-'15	4	12.3
	Tugela basin	'90-'15	4	12.3
Discharge (additional)	upper Po basin	'15-'17	8	2.2
Soil moisture content (additional)	Rhine basin	'13-'17	1	4.5
Total water storage anomaly (additional)	Rhine basin	'13-'17	4	3.3

**Table 3.** Number of observations and their average duration, per variable, region and period, used in the validation comparison. In the bottom part, information for the additional comparisons with a different spatiotemporal subselections is shown (see Technical Validation Section). For the discharge, evapotranspiration and soil moisture content anomaly variables, the number of observations indicates the number of observation stations (at every depth for the soil moisture content anomalies). For the total water storage anomaly variable, observations are aggregated for each region (see Technical Validation Section), resulting in a single observation for each of the four GRACE solutions (CRS spherical, GFZ spherical, JPL spherical and JPL mascon).

variable (Table 3). This sub-selection process ensures that every simulation is compared to the same set of observations in both temporal and spatial dimensions. The only exception is the soil moisture anomaly observations, as some simulations estimated soil moisture anomalies at greater depths than others. Therefore, more soil observations at depth could be included in these simulations, resulting in varying sets of soil moisture anomaly observations. Observations that contained less than two years of data during the common simulation period are excluded.

Not all simulations could be consistently combined in the comparison, as the common simulation period or geographical domain would have been too small (see Table 2). The Geoframe model simulations are only available for the upper Po basin, resulting in a common geographical domain of the upper Po. Additionally, the Geoframe and Parflow-CLM model simulations are only available after 2015 and 2013, respectively, whereas the PCR-GLOBWB model simulations are only available until 2015, resulting in a common simulation period of a year. Therefore, two additional comparisons are made with their own sub-selections (Table 3). First, a discharge comparison is conducted for the upper Po basin that includes the GEOframe model simulations and excludes the PCR-GLOBWB model simulations. Second, a soil moisture and total water storage anomaly comparison is conducted for the Rhine that includes the Parflow-CLM model simulations and excludes the PCR-GLOBWB model simulations.

**Performance Metrics.** Performance is evaluated using the Kling-Gupta Efficiency (KGE)<sup>127</sup> metric and its components. The KGE is calculated following Equation (1), where  $r$  is the correlation component (Equation (2)),  $\alpha$  is the variability ratio component (Equation (3)) and  $\beta$  is the bias ratio component (Equation (4)). Note that  $o$  denotes the observations and  $s$  denotes the simulations

$$KGE = 1 - \sqrt{(r - 1)^2 + (\alpha - 1)^2 + (\beta - 1)^2} \quad (1)$$

$$r = \frac{\text{cov}(o, s)}{\sigma_o \sigma_s} \quad (2)$$

$$\alpha = \frac{\sigma_s}{\sigma_o} \quad (3)$$

$$\beta = \frac{H_s}{H_o} \quad (4)$$

## Simulation performance

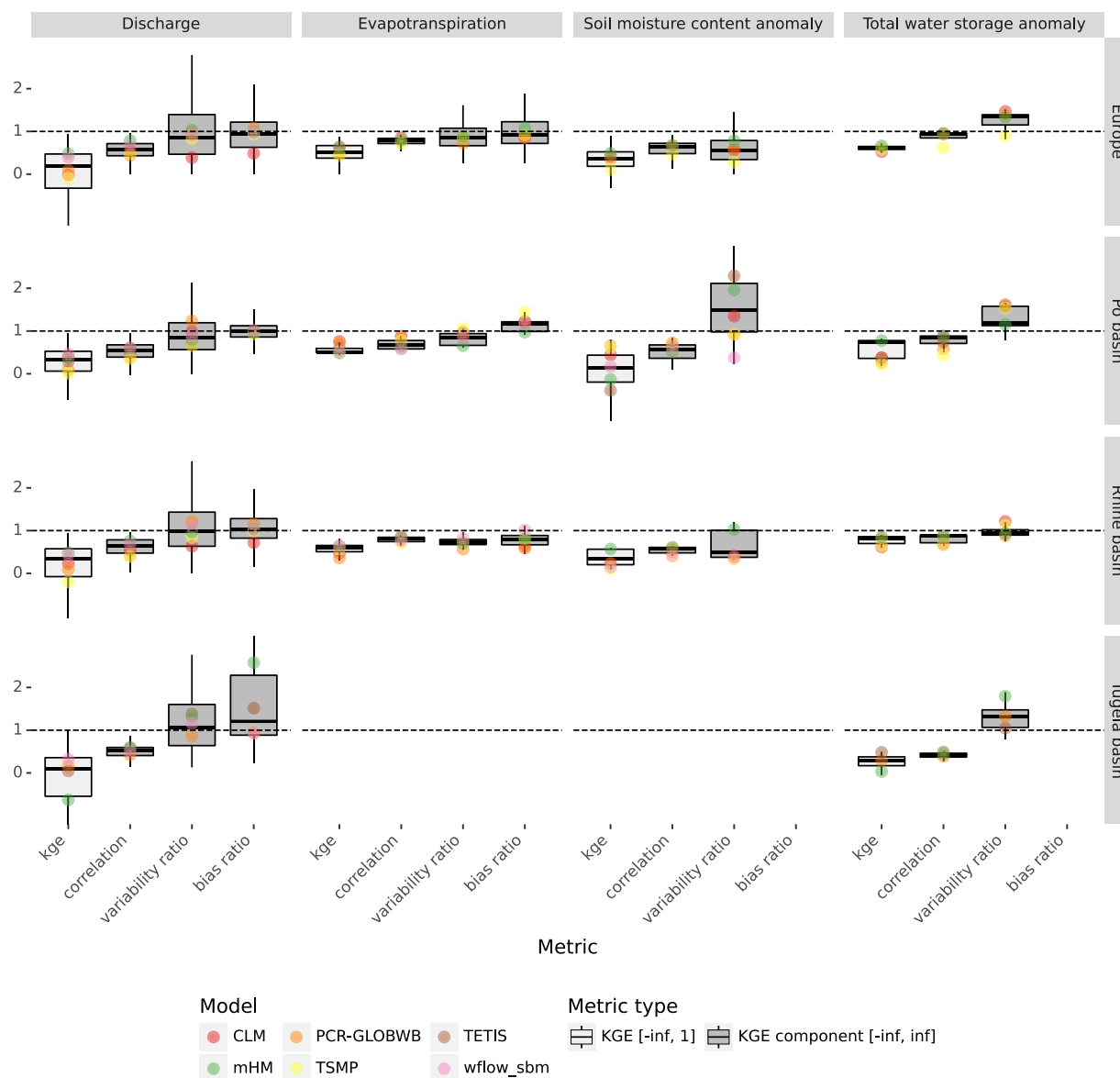


**Fig. 2** Simulated daily discharge, evapotranspiration, soil moisture anomaly and monthly total water storage anomaly performance for each region. Performance is measured by the Kling-Gupta efficiency (KGE) and its components, as shown on the x-axis. The KGE bias ratio is omitted for the anomalies, as the bias is zero by definition. The dashed horizontal line indicates the optimal performance value, whereas the box color indicates the performance range. Colored points indicate the median performance for each model. Note that some models include multiple simulations with different meteorology and resolution settings.

**Validation Results.** Figures 2 and 3 summarize the simulation performance across four regions and four variables. Additionally, maps of the spatial performance distribution and figures for the monthly deseasonalized performance are available in the Supplementary Information. In general, the simulations perform well compared to the observed data, although the performance differs between variables. The median Kling-Gupta Efficiency (KGE) falls within the range of 0.15 to 0.76 for discharge, soil moisture anomaly, evapotranspiration and total water storage anomaly, in that respective order. Moreover, the correlation between simulations and observations is good, with median correlations larger than 0.6 over all variables and regions.

Over all variables and regions, the median bias ratio (0.97) is generally better than the median variability ratio (0.84), indicating that the simulations are better at capturing the mean than the deviation in the observations. Additionally, over all variables, the median KGE in the Po and Rhine river basins (0.32 and 0.36, respectively) is generally better than in continental Europe and the Tugela river basin (0.23 and 0.17, respectively). This regional difference is likely related to the availability of observations and the subsequent higher-quality input data (e.g. meteorology and soil characteristics) for these regions.



## Additional simulation performance

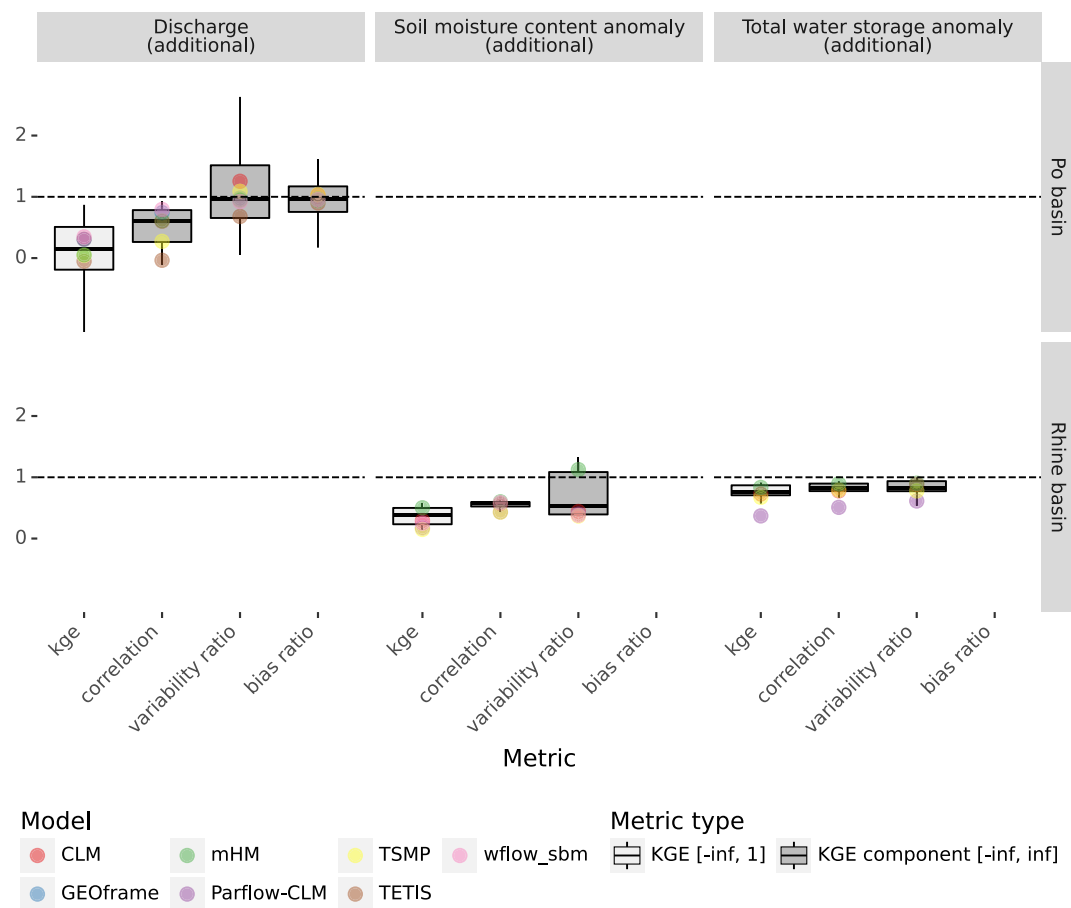


**Fig. 3** Additional simulated daily discharge, soil moisture anomaly and monthly total water storage anomaly performance for each region. Additional performances have a different spatiotemporal subselection (see Technical Validation Section). Performance is measured by the Kling-Gupta efficiency (KGE) and its components, as shown on the x-axis. The KGE bias ratio is omitted for the anomalies, as the bias is zero by definition. The dashed horizontal line indicates the optimal performance value, whereas the box color indicates the performance range. Colored points indicate the median performance for each model. Note that some models include multiple simulations with different meteorology and resolution settings.

Where the median values indicate the simulation performance, their variability indicates the uncertainty in the simulations. Here, we assess the uncertainty introduced by the model selection and region selection separately. For discharge, total water storage anomaly and soil moisture anomaly outputs, the model selection introduces the most variability. These variables show a larger median KGE interquartile range (1<sup>th</sup> to 3<sup>rd</sup> quantile) for each region encompassing all models (0.73, 0.18 and 0.34, respectively) than for each model containing all regions (0.71, 0.12 and 0.31, respectively). For discharge, the Tugela basin exhibits the most model-induced variability (0.9 interquartile range), whereas for total water storage and soil moisture anomaly, the Po basin exhibits the model-induced variability (0.4 and 0.6 interquartile range, respectively). We speculate that the reason for this model uncertainty is the presence or absence of lateral groundwater flow and human impact modules in the models. However, a harmonized model validation experiment is needed to confirm these speculations.

Conversely, for evapotranspiration outputs, the region selection introduces the most variability. This variable shows a larger median KGE interquartile range for each model encompassing all regions (0.26) than for each region containing all models (0.15). The same holds for the deseasonalized performance (see Supplementary Information). The reason for this regional uncertainty is likely because most models implement a similar evapotranspiration scheme that is strongly linked to meteorology. Therefore, regional uncertainties in meteorology are the main driver for uncertainties in evapotranspiration simulations.

### Usage Notes

Although each modeling group has stored their simulations on a public repository, all simulations are also referenced following the SpatioTemporal Asset Catalog (STAC) protocol on the 4DHydro open science catalog: [4dhydro.eu/catalog/](https://4dhydro.eu/catalog/). Simulations can be found under products and then under working package 2. This catalog ensures simulations are discoverable by end-users, both the scientific community and the general public.

## Code availability

Model code for our LSM/HMs are publicly available on GitHub: CLM<sup>128</sup>, GEOframe<sup>129</sup>, mHM<sup>48</sup>, Parflow<sup>130</sup>, PCR-GLOBWB<sup>131</sup>, TETIS<sup>132</sup>, TSMP<sup>133</sup> and wflow\_sbm<sup>134</sup>. Benchmark code (Python and Jupyter Notebook) related to the technical validation is publicly available on GitLab<sup>135</sup>.

Received: 12 December 2023; Accepted: 23 August 2024;

Published online: 17 September 2024

## References

- Bojinski, S. *et al.* The concept of essential climate variables in support of climate research, applications, and policy. *Bulletin of the American Meteorological Society* **95**, 1431–1443, <https://doi.org/10.1175/BAMS-D-13-00047.1> (2014).
- Global Climate Observing System (GCOS). About Essential Climate Variables. <https://gcos.wmo.int/en/essential-climate-variables/about> Accessed 2023-12-04 (2023).
- Global Climate Observing System (GCOS). Essential Climate Variables. <https://gcos.wmo.int/en/essential-climate-variables> Accessed 2023-12-04 (2023).
- Dee, D. *et al.* Toward a consistent reanalysis of the climate system. *Bulletin of the American Meteorological Society* **95**, 1235–1248, <https://doi.org/10.1175/BAMS-D-13-00043.1> (2014).
- Balmaseda, M. A. *et al.* The ocean reanalyses intercomparison project (ora-ip). *Journal of Operational Oceanography* **8**, s80–s97, <https://doi.org/10.1080/1755876X.2015.1022329> (2015).
- Barker Schaaf, C. *et al.* Terrestrial essential climate variables for climate change assessment, mitigation and adaptation. Tech. Rep., Food and Agriculture Organization of the United Nations (FAO), Rome (2008).
- Baatz, R. *et al.* Reanalysis in earth system science: Toward terrestrial ecosystem reanalysis. *Reviews of Geophysics* **59**, e2020RG000715, <https://doi.org/10.1029/2020RG000715> (2021).
- Baldocchi, D., Dralle, D., Jiang, C. & Ryu, Y. How much water is evaporated across California? a multiyear assessment using a biophysical model forced with satellite remote sensing data. *Water Resources Research* **55**, 2722–2741, <https://doi.org/10.1029/2018WR023884> (2019).
- Zink, M., Kumar, R., Cuntz, M. & Samaniego, L. A high-resolution dataset of water fluxes and states for Germany accounting for parametric uncertainty. *Hydrology and Earth System Sciences* **21**, 1769–1790, <https://doi.org/10.5194/hess-21-1769-2017> (2017).
- Gou, J. *et al.* Cnrnd v1.0: a high-quality natural runoff dataset for hydrological and climate studies in China. *Bulletin of the American Meteorological Society* **1–57** <https://doi.org/10.1175/BAMS-D-20-0094.1> (2021).
- Shrestha, P. *et al.* Towards improved simulations of disruptive reservoirs in global hydrological modelling. *Water Resources Research* (2023). Submitted. In revision (minor).
- Dickinson, R. E. *et al.* The community land model and its climate statistics as a component of the community climate system model. *Journal of Climate* **19**, 2302–2324, <https://doi.org/10.1175/JCLI3742.1> (2006).
- Collins, W. D. *et al.* The community climate system model version 3 (ccsm3). *Journal of Climate* **19**, 2122–2143, <https://doi.org/10.1175/JCLI3761.1> (2006).
- Oleson, K. W. *et al.* Improvements to the community land model and their impact on the hydrological cycle. *Journal of Geophysical Research: Biogeosciences* **113** <https://doi.org/10.1029/2007JG000563> (2008).
- Naz, B. S., Kollet, S. J., Franssen, H. J. H., Montzka, C. & Kurtz, W. A 3 km spatially and temporally consistent European daily soil moisture reanalysis from 2000 to 2015. *Scientific Data* **7** <https://doi.org/10.1038/s41597-020-0450-6> (2020).
- Lawrence, P. J. & Chase, T. N. Representing a new MODIS consistent land surface in the community land model (CLM 3.0). *Journal of Geophysical Research: Biogeosciences* **112**, <https://doi.org/10.1029/2006JG000168> (2007).
- Thornton, P. E. & Zimmermann, N. E. An improved canopy integration scheme for a land surface model with prognostic canopy structure. *Journal of Climate* **20**, 3902–3923, <https://doi.org/10.1175/JCLI4222.1> (2007).
- Lawrence, D. M., Thornton, P. E., Oleson, K. W. & Bonan, G. B. The partitioning of evapotranspiration into transpiration, soil evaporation, and canopy evaporation in a GCM: Impacts on land–atmosphere interaction. *Journal of Hydrometeorology* **8**, 862–880, <https://doi.org/10.1175/JHM596.1> (2007).
- Niu, G.-Y., Yang, Z.-L., Dickinson, R. E. & Gulden, L. E. A simple topmodel-based runoff parameterization (simtop) for use in global climate models. *Journal of Geophysical Research: Atmospheres* **110**, <https://doi.org/10.1029/2005JD006111> (2005).
- Niu, G.-Y., Yang, Z.-L., Dickinson, R. E., Gulden, L. E. & Su, H. Development of a simple groundwater model for use in climate models and evaluation with gravity recovery and climate experiment data. *Journal of Geophysical Research: Atmospheres* **112**, <https://doi.org/10.1029/2006JD007522> (2007).
- Niu, G.-Y. & Yang, Z.-L. Effects of frozen soil on snowmelt runoff and soil water storage at a continental scale. *Journal of Hydrometeorology* **7**, 937–952, <https://doi.org/10.1175/JHM538.1> (2006).
- Naz, B. S. *et al.* Improving soil moisture and runoff simulations at 3 km over Europe using land surface data assimilation. *Hydrology and Earth System Sciences* **23**, 277–301, <https://doi.org/10.5194/hess-23-277-2019> (2019).
- LIU, J.-G., JIA, B.-H., XIE, Z.-H. & SHI, C.-X. Improving the simulation of terrestrial water storage anomalies over China using a Bayesian model averaging ensemble approach. *Atmospheric and Oceanic Science Letters* **11**, 322–329, <https://doi.org/10.1080/16742834.2018.1484656> (2018).
- Lawrence, D. M. *et al.* Parameterization improvements and functional and structural advances in version 4 of the community land model. *Journal of Advances in Modeling Earth Systems* **3**, <https://doi.org/10.1029/2011MS00045> (2011).
- David, O. *et al.* A software engineering perspective on environmental modeling framework design: The object modeling system. *Environmental Modelling & Software* **39**, 201–213, <https://doi.org/10.1016/j.envsoft.2012.03.006> (2013).
- Tubini, N. & Rigon, R. Implementing the water, heat and transport model in GeoFrame (whetGeo-1d v1.0): algorithms, informatics, design patterns, open science features, and 1d deployment. *Geoscientific Model Development* **15**, 75–104, <https://doi.org/10.5194/gmd-15-75-2022> (2022).
- Formetta, G., Antonello, A., Franceschi, S., David, O. & Rigon, R. Hydrological modelling with components: A GIS-based open-source framework. *Environmental Modelling & Software* **55**, 190–200, <https://doi.org/10.1016/j.envsoft.2014.01.019> (2014).
- Serafin, F., David, O., Carlson, J. R., Green, T. R. & Rigon, R. Bridging technology transfer boundaries: Integrated cloud services deliver results of nonlinear process models as surrogate model ensembles. *Environmental Modelling & Software* **146**, 105231, <https://doi.org/10.1016/j.envsoft.2021.105231> (2021).
- Formetta, G., Mantilla, R., Franceschi, S., Antonello, A. & Rigon, R. The jgrass-newage system for forecasting and managing the hydrological budgets at the basin scale: models of flow generation and propagation/routing. *Geoscientific Model Development* **4**, 943–955, <https://doi.org/10.5194/gmd-4-943-2011> (2011).
- Formetta, G., Kampf, S. K., David, O. & Rigon, R. Snow water equivalent modeling components in newage-jgrass. *Geoscientific Model Development* **7**, 725–736, <https://doi.org/10.5194/gmd-7-725-2014> (2014).
- Bottazzi, M. *et al.* Comparing evapotranspiration estimates from the GeoFrame-prospéro model with Penman–Monteith and Priestley–Taylor approaches under different climate conditions. *Water* **13**, <https://doi.org/10.3390/w13091221> (2021).
- Abera, W., Antonello, A., Franceschi, S., Formetta, G. & Rigon, R. *The uDig Spatial Toolbox for hydro-geomorphic analysis*, chap. 2, 1–19 (British Society of Geomorphology, 2014).

33. Bancheri, M. *et al.* The design, deployment, and testing of kriging models in geoframe with sik-0.9.8. *Geoscientific Model Development* **11**, 2189–2207, <https://doi.org/10.5194/gmd-11-2189-2018> (2018).
34. Abera, W., Formetta, G., Brocca, L. & Rigon, R. Modeling the water budget of the upper blue Nile basin using the jgrass-newage model system and satellite data. *Hydrology and Earth System Sciences* **21**, 3145–3165, <https://doi.org/10.5194/hess-21-3145-2017> (2017).
35. Rigon, R. *et al.* Hess opinions: Participatory digital earth twin hydrology systems (darts) for everyone – a blueprint for hydrologists. *Hydrology and Earth System Sciences* **26**, 4773–4800, <https://doi.org/10.5194/hess-26-4773-2022> (2022).
36. Azimi, S. *et al.* On understanding mountainous carbonate basins of the mediterranean using parsimonious modeling solutions. *Hydrology and Earth System Sciences* **27**, 4485–4503, <https://doi.org/10.5194/hess-27-4485-2023> (2023).
37. Samaniego, L., Kumar, R. & Attinger, S. Multiscale parameter regionalization of a grid-based hydrologic model at the mesoscale. *Water Resources Research* **46**, <https://doi.org/10.1029/2008WR007327> (2010).
38. Kumar, R., Samaniego, L. & Attinger, S. Implications of distributed hydrologic model parameterization on water fluxes at multiple scales and locations. *Water Resources Research* **49**, 360–379, <https://doi.org/10.1029/2012WR012195> (2013).
39. Rakovec, O., Kumar, R., Attinger, S. & Samaniego, L. Improving the realism of hydrologic model functioning through multivariate parameter estimation. *Water Resources Research* **52**, 7779–7792, <https://doi.org/10.1002/2016WR019430> (2016).
40. Thober, S. *et al.* The multiscale routing model mrm v1.0: simple river routing at resolutions from 1 to 50 km. *Geoscientific Model Development* **12**, <https://doi.org/10.5194/gmd-12-2501-2019> (2019).
41. Kumar, R., Livneh, B. & Samaniego, L. Toward computationally efficient large-scale hydrologic predictions with a multiscale regionalization scheme. *Water Resources Research* **49**, 5700–5714, <https://doi.org/10.1002/wrcr.20431> (2013).
42. Thober, S. *et al.* Multi-model ensemble projections of European river floods and high flows at 1.5, 2, and 3 degrees global warming. *Environmental Research Letters* **13**, 014003, <https://doi.org/10.1088/1748-9326/aa9e35> (2018).
43. Samaniego, L. *et al.* Anthropogenic warming exacerbates European soil moisture droughts. *Nature Climate Change* **5**, 1117–1121, <https://doi.org/10.1038/s41558-018-0138-5> (2018).
44. Marx, A. *et al.* Climate change alters low flows in Europe under global warming of 1.5, 2, and 3 °C. *Hydrology and Earth System Sciences* **22**, 1017–1032, <https://doi.org/10.5194/hess-22-1017-2018> (2018).
45. Wanders, N. *et al.* Development and evaluation of a pan-European multimodel seasonal hydrological forecasting system. *Journal of Hydrometeorology* **20**, 99–115, <https://doi.org/10.1175/JHM-D-18-0040.1> (2019).
46. Samaniego, L. *et al.* Hydrological forecasts and projections for improved decision-making in the water sector in Europe. *Bulletin of the American Meteorological Society* **100**, 2451–2472, <https://doi.org/10.1175/BAMS-D-17-0274.1> (2019).
47. Zink, M. *et al.* The German drought monitor. *Environmental Research Letters* **11**, 074002, <https://doi.org/10.1088/1748-9326/11/7/074002> (2016).
48. Samaniego, L. *et al.* mhm-ufz/mhm: v5.13.1 <https://doi.org/10.5281/zenodo.8279545> (2023).
49. Pohl, F. *et al.* Long-term daily hydrometeorological drought indices, soil moisture, and evapotranspiration for ICOS sites. *Scientific Data* **10**, 281, <https://doi.org/10.1038/s41597-023-02192-1> (2023).
50. Kollet, S. J. & Maxwell, R. M. Integrated surface–groundwater flow modeling: A free-surface overland flow boundary condition in a parallel groundwater flow model. *Advances in Water Resources* **29**, 945–958, <https://doi.org/10.1016/j.advwatres.2005.08.006> (2006).
51. Maxwell, R. M. A terrain-following grid transform and preconditioner for parallel, large-scale, integrated hydrologic modeling. *Advances in Water Resources* **53**, 109–117, <https://doi.org/10.1016/j.advwatres.2012.10.001> (2013).
52. Dai, Y. *et al.* The common land model. *Bulletin of the American Meteorological Society* **84**, 1013–1024, <https://doi.org/10.1175/BAMS-84-8-1013> (2003).
53. Maxwell, R. M., Condon, L. E. & Kollet, S. J. A high-resolution simulation of groundwater and surface water over most of the continental US with the integrated hydrologic model Parflow v3. *Geoscientific Model Development* **8**, 923–937, <https://doi.org/10.5194/gmd-8-923-2015> (2015).
54. Kuffour, B. N. O. *et al.* Simulating coupled surface–subsurface flows with Parflow v3.5.0: capabilities, applications, and ongoing development of an open-source, massively parallel, integrated hydrologic model. *Geoscientific Model Development* **13**, 1373–1397, <https://doi.org/10.5194/gmd-13-1373-2020> (2020).
55. Belleflamme, A. *et al.* Hydrological forecasting at impact scale: the integrated Parflow hydrological model at 0.6 km for climate resilient water resource management over Germany. *Frontiers in Water* **5**, <https://doi.org/10.3389/frwa.2023.1183642> (2023).
56. van Beek, R. & Bierkens, M. F. The global hydrological model PCR-GLOBWB: Conceptualization, parameterization and verification. Tech. Rep., Department of Physical Geography, Utrecht University, Utrecht, the Netherlands Accessed 2023-11-28 (2009).
57. Sutanudjaja, E. H. *et al.* PCR-GLOBWB 2: a 5 arcmin global hydrological and water resources model. *Geoscientific Model Development* **11**, 2429–2453, <https://doi.org/10.5194/gmd-11-2429-2018> (2018).
58. Wada, Y., Wisser, D. & Bierkens, M. F. Global modeling of withdrawal, allocation and consumptive use of surface water and groundwater resources. *Earth System Dynamics* **5**, 15–40, <https://doi.org/10.5194/esd-5-15-2014> (2014).
59. van Beek, L. P. H., Wada, Y. & Bierkens, M. F. P. Global monthly water stress: 1. water balance and water availability. *Water Resources Research* **47**, <https://doi.org/10.1029/2010WR009791> (2011).
60. Wada, Y. *et al.* Global monthly water stress: 2. water demand and severity of water stress. *Water Resources Research* **47**, <https://doi.org/10.1029/2010WR009792> (2011).
61. van Beek, L. P., Eikelboom, T., van Vliet, M. T. & Bierkens, M. F. A physically based model of global freshwater surface temperature. *Water Resources Research* **48**, <https://doi.org/10.1029/2012WR011819> (2012).
62. Sutanudjaja, E., Van Beek, L., De Jong, S., Van Geer, F. & Bierkens, M. Calibrating a large-extent high-resolution coupled groundwater–land surface model using soil moisture and discharge data. *Water Resources Research* **50**, 687–705, <https://doi.org/10.1002/2013WR013807> (2014).
63. de Graaf, I. D., Sutanudjaja, E., Van Beek, L. & Bierkens, M. A high-resolution global-scale groundwater model. *Hydrology and Earth System Sciences* **19**, 823–837, <https://doi.org/10.5194/hess-19-823-2015> (2015).
64. Van Vliet, M. *et al.* Multi-model assessment of global hydropower and cooling water discharge potential under climate change. *Global Environmental Change* **40**, 156–170, <https://doi.org/10.1016/j.gloenvcha.2016.07.007> (2016).
65. de Graaf, I. E., Gleeson, T., Van Beek, L., Sutanudjaja, E. H. & Bierkens, M. F. Environmental flow limits to global groundwater pumping. *Nature* **574**, 90–94, <https://doi.org/10.1038/s41586-019-1594-4> (2019).
66. Verkaik, J., Sutanudjaja, E. H., Oude Essink, G. H., Lin, H. X. & Bierkens, M. F. Globgm v1.0: a parallel implementation of a 30 arcsec PCR-GLOBWB-modflow global-scale groundwater model. *Geoscientific Model Development Discussions* **2022**, 1–27, <https://doi.org/10.5194/gmd-2022-226> (2022).
67. Hoch, J. M., Sutanudjaja, E. H., Wanders, N., Van Beek, R. L. & Bierkens, M. F. Hyper-resolution PCR-GLOBWB: opportunities and challenges from refining model spatial resolution to 1 km over the European continent. *Hydrology and Earth System Sciences* **27**, 1383–1401, <https://doi.org/10.5194/hess-27-1383-2023> (2023).
68. Francés, F., Vélez, J. I. & Vélez, J. J. Split-parameter structure for the automatic calibration of distributed hydrological models. *Journal of Hydrology* **332**, 226–240, <https://doi.org/10.1016/j.jhydrol.2006.06.032> (2007).
69. Vélez, J. J., Puricelli, M., López Unzu, F. & Francés, F. Parameter extrapolation to ungauged basins with a hydrological distributed model in a regional framework. *Hydrology and Earth System Sciences* **13**, 229–246, <https://doi.org/10.5194/hess-13-229-2009> (2009).
70. Bussi, G., Francés, F., Horel, E., López-Tarazón, J. A. & Batalla, R. J. Modelling the impact of climate change on sediment yield in a highly erodible Mediterranean catchment. *Journal of Soils and Sediments* **14**, 1921–1937, <https://doi.org/10.1007/s11368-014-0956-7> (2014).

71. Ruiz-Villanueva, V., Bussi, G., Francés, F. & Bréthaut, C. Climate change impacts on discharges of the rhone river in lyon by the end of the 21st century: model results and implications. *Regional Environmental Change* **15**, 505–515, <https://doi.org/10.1007/s10113-014-0707-8> (2015).
72. Siswanto, S. Y. & Francés, F. How land use/land cover changes can affect water, flooding and sedimentation in a tropical watershed: a case study using distributed modeling in the upper citarum watershed, indonesia. *Environmental Earth Sciences* **78**, <https://doi.org/10.1007/s12665-019-8561-0> (2019).
73. Puertes, C. *et al.* Improving the modelling and understanding of carbon-nitrogen-water interactions in a semiarid mediterranean oak forest. *Ecological Modelling* **420**, 108976, <https://doi.org/10.1016/j.ecolmodel.2020.108976> (2020).
74. Pool, S. *et al.* From flood to drip irrigation under climate change: Impacts on evapotranspiration and groundwater recharge in the mediterranean region of valencia (spain). *Earth's Future* **9**, <https://doi.org/10.1029/2020EF001859> (2021).
75. Echeverría, C. *et al.* Assessment of remotely sensed near-surface soil moisture for distributed eco-hydrological model implementation. *Water* **11**, 2613–2619, <https://doi.org/10.3390/w11122613> (2019).
76. Gomis-Cebolla, J., Garcia-Arias, A., Perpinyà-Vallès, M. & Francés, F. Evaluation of sentinel-1, smap and smos surface soil moisture products for distributed eco-hydrological modelling in mediterranean forest basins. *Journal of Hydrology* **608**, 127569, <https://doi.org/10.1016/j.jhydrol.2022.127569> (2022).
77. Gasper, F. *et al.* Implementation and scaling of the fully coupled terrestrial systems modeling platform (terrsysmp v1. 0) in a massively parallel supercomputing environment—a case study on juqueen (ibm blue gene/q). *Geoscientific model development* **7**, 2531–2543, <https://doi.org/10.5194/gmd-7-2531-2014> (2014).
78. Shrestha, P., Sulis, M., Masbou, M., Kollet, S. & Simmer, C. A scale-consistent terrestrial systems modeling platform based on cosmo, clm, and parflow. *Monthly weather review* **142**, 3466–3483, <https://doi.org/10.1175/MWR-D-14-00029.1> (2014).
79. Baldauf, M. *et al.* Operational convective-scale numerical weather prediction with the cosmo model: Description and sensitivities. *Monthly Weather Review* **139**, 3887–3905, <https://doi.org/10.1175/MWR-D-10-05013.1> (2011).
80. Valcke, S. The oasis3 coupler: A european climate modelling community software. *Geoscientific Model Development* **6**, 373–388, <https://doi.org/10.5194/gmd-6-373-2013> (2013).
81. Furusho-Percot, C. *et al.* Pan-european groundwater to atmosphere terrestrial systems climatology from a physically consistent simulation. *Scientific data* **6**, 320, <https://doi.org/10.1038/s41597-019-0328-7> (2019).
82. Li, F., Kurtz, W., Hung, C. P., Vereecken, H. & Hendricks Franssen, H.-J. Water table depth assimilation in integrated terrestrial system models at the larger catchment scale. *Frontiers in water* **5**, 1150999, <https://doi.org/10.3389/frwa.2023.1150999> (2023).
83. Hartick, C., Furusho-Percot, C., Goergen, K. & Kollet, S. An interannual probabilistic assessment of subsurface water storage over europe using a fully coupled terrestrial model. *Water Resources Research* **57**, e2020WR027828, <https://doi.org/10.1029/2020WR027828> (2021).
84. van Verseveld, W. J. *et al.* Wflow\_sbm v0.7.3, a spatially distributed hydrologic model: from global data to local applications. *Geoscientific Model Development* **17**, 3199–3234, <https://doi.org/10.5194/gmd-17-3199-2024> (2024).
85. Vertessy, R. A. & Elsenbeer, H. Distributed modeling of storm flow generation in an amazonian rain forest catchment: Effects of model parameterization. *Water Resources Research* **35**, 2173–2187, <https://doi.org/10.1029/1999WR900051> (1999).
86. Eilander, D. *et al.* Hydromt: Automated and reproducible model building and analysis. journal of open source software. *Journal of Open Source Software* **8**, 2173–2187, <https://doi.org/10.21105/joss.04897> (2023).
87. Eilander, D. *et al.* A hydrography upscaling method for scale-invariant parameterization of distributed hydrological models. *Hydrology and Earth System Sciences* **25**, 5287–5313, <https://doi.org/10.5194/hess-25-5287-2021> (2021).
88. Imhoff, R. O., van Verseveld, W. J., van Osnabrugge, B. & Weerts, A. H. Scaling Point-Scale (Pedo)transfer Functions to Seamless Large-Domain Parameter Estimates for High-Resolution Distributed Hydrologic Modeling: An Example for the Rhine River. *Water Resources Research* **56**, e2019WR026807, <https://doi.org/10.1029/2019WR026807> (2020).
89. López López, P. *et al.* Improved large-scale hydrological modelling through the assimilation of streamflow and downscaled satellite soil moisture observations. *Hydrology and Earth System Sciences* **20**, 3059–3076, <https://doi.org/10.5194/hess-20-3059-2016> (2016).
90. Rusli, S., Bense, V., Taufiq, A. & Weerts, A. Quantifying basin-scale changes in groundwater storage using grace and one-way coupled hydrological and groundwater flow model in the data-scarce bandung groundwater basin, indonesia. *Groundwater for Sustainable Development* **22**, 100953, <https://doi.org/10.1016/j.gsd.2023.100953> (2023).
91. van der Laan, E., Hazenberg, P. & Weerts, A. H. Simulation of long-term storage dynamics of headwater reservoirs across the globe using public cloud computing infrastructure. *Science of The Total Environment* **931**, 172678, <https://doi.org/10.1016/j.scitotenv.2024.172678> (2024).
92. Aerts, J. P. *et al.* Large-sample assessment of varying spatial resolution on the streamflow estimates of the wflow\_sbm hydrological model. *Hydrology and Earth System Sciences* **26**, 4407–4430, <https://doi.org/10.5194/hess-26-4407-2022> (2022).
93. Priestley, C. H. B. & Taylor, R. J. On the assessment of surface heat flux and evaporation using large-scale parameters. *Monthly weather review* **100**, 81–92, [https://doi.org/10.1175/1520-0493\(1972\)100<0081:O'TAOSH>2.3.CO;2](https://doi.org/10.1175/1520-0493(1972)100<0081:O'TAOSH>2.3.CO;2) (1972).
94. Hargreaves, G. H. & Samani, Z. A. Reference crop evapotranspiration from temperature. *Applied engineering in agriculture* **1**, 96–99, <https://doi.org/10.13031/2013.26773> (1985).
95. Allen, R. G. *et al.* Crop evapotranspiration-guidelines for computing crop water requirements - fao irrigation and drainage paper 56. Tech. Rep., Food and Agriculture Organization of the United Nations (FAO) (1998).
96. de Bruin, H. D., Trigo, I., Bosveld, F. & Meirink, J. A thermodynamically based model for actual evapotranspiration of an extensive grass field close to fao reference, suitable for remote sensing application. *Journal of Hydrometeorology* **17**, 1373–1382, <https://doi.org/10.1175/JHM-D-15-0006.1> (2016).
97. Haylock, M. *et al.* A european daily high-resolution gridded data set of surface temperature and precipitation for 1950–2006. *Journal of Geophysical Research: Atmospheres* **113**, <https://doi.org/10.1029/2008JD010201> (2008).
98. Hofstra, N., Haylock, M., New, M. & Jones, P. D. Testing E-OBS European high-resolution gridded data set of daily precipitation and surface temperature. *Journal of Geophysical Research: Atmospheres* **114**, <https://doi.org/10.1029/2009JD011799> (2009).
99. Klein Tank, A. *et al.* Daily dataset of 20th-century surface air temperature and precipitation series for the european climate assessment. *International Journal of Climatology: A Journal of the Royal Meteorological Society* **22**, 1441–1453, <https://doi.org/10.1002/joc.773> (2002).
100. Klok, E. & Klein Tank, A. Updated and extended european dataset of daily climate observations. *International Journal of Climatology: A Journal of the Royal Meteorological Society* **29**, 1182–1191, <https://doi.org/10.1002/joc.1779> (2009).
101. Thiemi, V. *et al.* Emo-5: a high-resolution multi-variable gridded meteorological dataset for europe. *Earth System Science Data* **14**, 3249–3272, <https://doi.org/10.5194/essd-14-3249-2022> (2022).
102. Hersbach, H. *et al.* The era5 global reanalysis. *Quarterly Journal of the Royal Meteorological Society* **146**, 1999–2049, <https://doi.org/10.1002/qj.3803> (2020).
103. Dee, D. P. *et al.* The era-interim reanalysis: Configuration and performance of the data assimilation system. *Quarterly Journal of the royal meteorological society* **137**, 553–597, <https://doi.org/10.1002/qj.828> (2011).
104. Owens, R. G. & Hewson, T. D. Ecmwf forecast user guide. Tech. Rep., European Centre for Medium-Range Weather Forecasts (ECMWF) <https://doi.org/10.21957/m1cs7h> (2018).
105. Urraca, R. *et al.* Evaluation of global horizontal irradiance estimates from era5 and cosmo-rea6 reanalyses using ground and satellite-based data. *Solar Energy* **164**, 339–354, <https://doi.org/10.1016/j.solener.2018.02.059> (2018).



106. Centro Funzionale Regione autonoma Valle D'Aosta. Discharge and meteorological dataset. <https://presidi2.regione.vda.it/str-dataview> Accessed 2023-07-28 (2023).
107. The Global Runoff Data Centre. GRDC discharge dataset. <https://www.bafg.de/GRDC/> Accessed 2023-07-17 (2023).
108. Klingler, C., Schulz, K. & Herrnegger, M. Lamah-ce: Large-sample data for hydrology and environmental sciences for central europe. *Earth System Science Data* **13**, 4529–4565, <https://doi.org/10.5194/essd-13-4529-2021> (2021).
109. Coxon, G. *et al.* Camels-gb: hydrometeorological time series and landscape attributes for 671 catchments in great britain. *Earth System Science Data* **12**, 2459–2483, <https://doi.org/10.5194/essd-12-2459-2020> (2020).
110. Höge, M. *et al.* Camels-ch: hydro-meteorological time series and landscape attributes for 331 catchments in hydrologic switzerland. *Earth System Science Data Discussions* **2023**, 1–46, <https://doi.org/10.5194/essd-2023-127> (2023).
111. Dati Ambientali Emilia-Romagna. DAER discharge dataset. <https://webbook.arpae.it/indicatore/Portata-dei-fiumi-00001/?id=46803a8c-c127-11e2-9a51-11c9866a0f33> Accessed 2023-06-26 (2023).
112. Department Water and Sanitation of the Republic of South Africa (DWS). DWS discharge dataset. <https://www.dws.gov.za/> Accessed 2020-04-14 (2023).
113. L'Agenzia Regionale per la Protezione Ambientale del Lombardia. Discharge dataset. <https://idro.arpalombardia.it/it/map/sidro/> Accessed 2023-07-28 (2023).
114. L'Agenzia Regionale per la Protezione Ambientale del Piemonte. Discharge and meteorological dataset. [https://www.arpa.piemonte.it/rischi\\_naturali/snippets\\_arpa\\_graphs/map\\_meteorweb/?rete=stazione\\_meteorologica](https://www.arpa.piemonte.it/rischi_naturali/snippets_arpa_graphs/map_meteorweb/?rete=stazione_meteorologica) Accessed 2023-07-28 (2023).
115. Pastorello, G. *et al.* The fluxnet2015 dataset and the oneflux processing pipeline for eddy covariance data. *Scientific data* **7**, 225, <https://doi.org/10.1038/s41597-020-0534-3> (2020).
116. International Soil Moisture Network. ISMN soil moisture dataset. <https://ismn.earth/> Accessed 2023-07-25 (2023).
117. Dorigo, W. *et al.* The international soil moisture network: serving earth system science for over a decade. *Hydrology and earth system sciences* **25**, 5749–5804, <https://doi.org/10.5194/hess-25-5749-2021> (2021).
118. Landerer, F. W. & Swenson, S. Accuracy of scaled grace terrestrial water storage estimates. *Water resources research* **48** <https://doi.org/10.1029/2011WR011453> (2012).
119. Landerer, F. JPL TELLUS GRACE Level-3 Monthly Land Water-Equivalent-Thickness Surface Mass Anomaly Release 6.0 version 04 Accessed 2023-07-24 <https://doi.org/10.5067/TELND-3AJ64> (2021).
120. Landerer, F. JPL TELLUS GRACE-FO Level-3 Monthly Land Water-Equivalent-Thickness Surface Mass Anomaly Release 6.1 version 04 Accessed 2023-07-24 <https://doi.org/10.5067/GFLND-3J614> (2023).
121. Wiese, D. N., Yuan, D.-N., Boening, C., Landerer, F. W. & Watkins, M. M. JPL GRACE and GRACE-FO Mascon Ocean, Ice, and Hydrology Equivalent Water Height Coastal Resolution Improvement (CRI) Filtered Release 06.1 Version 03 Accessed 2023-08-23, <https://doi.org/10.5067/TEMSC-3JC63> (2023).
122. Landerer, F. CSR TELLUS GRACE Level-3 Monthly Land Water-Equivalent-Thickness Surface Mass Anomaly Release 6.0 version 04 Accessed 2023-07-24, <https://doi.org/10.5067/TELND-3AC64> (2021).
123. Landerer, F. CSR TELLUS GRACE-FO Level-3 Monthly Land Water-Equivalent-Thickness Surface Mass Anomaly Release 6.1 version 04 Accessed 2023-07-24, <https://doi.org/10.5067/GFLND-3C614> (2023).
124. Landerer, F. GFZ TELLUS GRACE Level-3 Monthly Land Water-Equivalent-Thickness Surface Mass Anomaly Release 6.0 version 04 Accessed 2023-07-24, <https://doi.org/10.5067/TELND-3AG64> (2021).
125. Landerer, F. GFZ TELLUS GRACE-FO Level-3 Monthly Land Water-Equivalent-Thickness Surface Mass Anomaly Release 6.1 version 04 Accessed 2023-07-24, <https://doi.org/10.5067/GFLND-3G614> (2023).
126. Humphrey, V., Rodell, M. & Eicker, A. Using satellite-based terrestrial water storage data: A review. *Surveys in Geophysics* **44**, 1489–1517, <https://doi.org/10.1007/s10712-022-09754-9> (2023).
127. Gupta, H. V. & Kling, H. On typical range, sensitivity, and normalization of mean squared error and nash-sutcliffe efficiency type metrics. *Water Resources Research* **47** <https://doi.org/10.1029/2011WR010962> (2011).
128. Oleson, K. *et al.* CLM3.5. <https://github.com/HPSCTerrSys/CLM3.5> (2023).
129. Formetta, G., Bancheri, M., Tubini, N., Andreis, D. & Morlot, M. GEOframe: Components Development. <https://github.com/geoframecomponents> (2023).
130. Smith, S. *et al.* parflow. <https://github.com/parflow/parflow> (2023).
131. Sutanudjaja, E. H. *et al.* PCR-GLOBWB model. [https://github.com/UU-Hydro/PCR-GLOBWB\\_model](https://github.com/UU-Hydro/PCR-GLOBWB_model) Accessed 2023-07-23 (2023).
132. Universitat Politècnica de València. TETIS: Conceptual and distributed hydrological model V9.1. <http://lluvia.dihma.upv.es/ES/software/software.html> (1995).
133. Keller, J. *et al.* TSMP. <https://github.com/HPSCTerrSys/TSMP> (2023).
134. van Verseveld, W. *et al.* Wflow.jl (v0.7.3). <https://doi.org/10.5281/zenodo.10495638> (2024).
135. Droppers, B. 4dHydro WP2 benchmark. <https://codebase.helmholtz.cloud/4dhydro/wp2/benchmark> Accessed 2024-06-08 (2024).
136. Food and Agriculture Organization of the United Nation (FAO). Digital Soil Map of the World (DSMW). [https://data.apps.fao.org/map/catalog/srv/eng/catalog\\_search#/metadata/446ed430-8383-11db-b9b2-000d939bc5d8](https://data.apps.fao.org/map/catalog/srv/eng/catalog_search#/metadata/446ed430-8383-11db-b9b2-000d939bc5d8) (2007).
137. Friedl, M. A. *et al.* Global land cover mapping from modis: algorithms and early results. *Remote sensing of Environment* **83**, 287–302, [https://doi.org/10.1016/S0034-4257\(02\)00078-0](https://doi.org/10.1016/S0034-4257(02)00078-0) (2002).
138. Hengl, T. *et al.* SoilGrids250m: Global gridded soil information based on machine learning. *PLoS One* **12**, e0169748, <https://doi.org/10.1371/journal.pone.0169748> (2017).
139. Danielson, J. J. *et al.* Global multi-resolution terrain elevation data 2010 (gmtded2010) <https://doi.org/10.3133/ofr20111073> (2011).
140. Lehner, B., Verdin, K. & Jarvis, A. New global hydrography derived from spaceborne elevation data. *Eos, Transactions American Geophysical Union* **89**, 93–94, <https://doi.org/10.1029/2008EO100001> (2008).
141. European Space Agency (ESA), Universit Catholique de Louvain. Global Land Cover Map for 2009. [http://due.esrin.esa.int/files/Globcover2009\\_V2.3\\_Global\\_zip](http://due.esrin.esa.int/files/Globcover2009_V2.3_Global_zip) (2009).
142. Tucker, C. J., Pinzon, J. E. & Brown, M. E. Global inventory modeling and mapping studies (gimms). <http://iridl.ldeo.columbia.edu/SOURCES/UMD/GLCF/GIMMS/NDVIg/global/> (2004).
143. Hartmann, J. & Moosdorf, N. Global Lithological Map Database v1.0 (gridded to 0.5 degree spatial resolution) (2012). Supplement to: Hartmann, Jens; Moosdorf, Nils (2012): The new global lithological map database GLiM: A representation of rock properties at the Earth surface. *Geochemistry, Geophysics, Geosystems*, **13**, Q12004, <https://doi.org/10.1029/2012GC004370>.
144. Zhang, Y. & Schaap, M. G. Weighted recalibration of the rosetta pedotransfer model with improved estimates of hydraulic parameter distributions and summary statistics (rosetta3). *Journal of Hydrology* **547**, 39–53, <https://doi.org/10.1016/j.jhydrol.2017.01.004> (2017).
145. European Environment Agency (EEA). Copernicus Land Monitoring Service 2018: Corine Land Cover (CLC) 2018, version 2020\_20u1 <https://doi.org/10.2909/960998c1-1870-4e82-8051-6485205ebbac> (2018).
146. Duscher, K. *et al.* The gis layers of the” international hydrogeological map of europe 1: 1,500,000” in a vector format. *Hydrogeology journal* **23**, 1867, <https://doi.org/10.1007/s10040-015-1296-4> (2015).
147. Gesch, D. B., Verdin, K. L. & Greenlee, S. K. New land surface digital elevation model covers the earth. *Eos, Transactions American Geophysical Union* **80**, 69–70, <https://doi.org/10.1029/99EO00050> (1999).
148. Verdin, K. & Greenlee, S. Development of continental scale digital elevation models and extraction of hydrographic features. In *Third International Conference/Workshop on Integrating GIS and Environmental Modeling, Santa Fe, New Mexico*, 21–26 (National Center for Geographic Information and Analysis, Santa Barbara, California, 1996).



149. Loveland, T. R. *et al.* Development of a global land cover characteristics database and igbp discover from 1 km avhrr data. *International journal of remote sensing* **21**, 1303–1330, <https://doi.org/10.1080/014311600210191> (2000).
150. Gleeson, T., Moosdorf, N., Hartmann, J. & van Beek, L. V. A glimpse beneath earth's surface: Global hydrogeology maps (glhyps) of permeability and porosity. *Geophysical Research Letters* **41**, 3891–3898, <https://doi.org/10.1002/2014GL059856> (2014).
151. Lehner, B. & Döll, P. Development and validation of a global database of lakes, reservoirs and wetlands. *Journal of hydrology* **296**, 1–22, <https://doi.org/10.1016/j.jhydrol.2004.03.028> (2004).
152. Portmann, F. T., Siebert, S. & Döll, P. Mirca2000—global monthly irrigated and rainfed crop areas around the year 2000: A new high-resolution data set for agricultural and hydrological modeling. *Global biogeochemical cycles* **24** <https://doi.org/10.1029/2008GB003435> (2010).
153. Lehner, B. *et al.* High-resolution mapping of the world's reservoirs and dams for sustainable river-flow management. *Frontiers in Ecology and the Environment* **9**, 494–502, <https://doi.org/10.1890/100125> (2011).
154. Food and Agriculture Organization of the United Nation (FAO). Soil Map of the World (DSMW). <https://www.fao.org/soils-portal/soil-survey/soil-maps-and-databases/faounesco-soil-map-of-the-world/en/> (1988).
155. Yamazaki, D. *et al.* MERIT Hydro: A high-resolution global hydrography map based on latest topography dataset. *Water Resources Research* **55**, 5053–5073, <https://doi.org/10.1029/2019WR024873> (2019).
156. Buchhorn, M. *et al.* Copernicus Global Land Service: Land cover 100m, epoch 2015, globe (version v2.0.2) <https://doi.org/10.5281/zenodo.3243509> (2019).
157. Myneni, R. B., Knyazikhin, Y. & Park, T. MCD15A3H MODIS/Terra+Aqua Leaf Area Index/FPAR 4-day L4 Global 500m SIN Grid V006, <https://doi.org/10.5067/MODIS/MCD15A3H.006> (2015).
158. Messenger, M. L., Lehner, B., Grill, G., Nedeva, L. & Schmitt, O. Estimating the volume and age of water stored in global lakes using a geo-statistical approach. *Nature Communications* **7**, <https://doi.org/10.1038/ncomms13603> (2016).
159. RGI Consortium. Randolph glacier inventory - A dataset of global glacier outlines: Version 6.0. <https://nsidc.org/data/nsidc-0770/versions/6> (2017).
160. Raup, B. H. *et al.* The GLIMS geospatial glacier database: A new tool for studying glacier change. *Global and Planetary Change* **56**, 101–110, <https://doi.org/10.1016/j.gloplacha.2006.07.018> (2007).
161. Fischer, M., Huss, M., Barboux, C. & Hoelzle, M. The new Swiss glacier inventory SGI2010: Relevance of using high-resolution source data in areas dominated by very small glaciers. *Arctic, Antarctic, and Alpine Research* **46**, 933–945, <https://doi.org/10.1657/1938-4246-46.4.933> (2007).
162. Kollet, S. *et al.* FZJ hydrological variables data collection for the ESA 4DHydro project. <https://datapub.fz-juelich.de/slots/4DHydro/> (2023).
163. Azimi, S. & Rigon, R. GEOframe 4DHydro simulations <https://doi.org/10.17605/OSF.IO/7NY3V> (2023).
164. Rakovec, O. & Samaniego, L. 4DHydro mHM Tier 1 simulations <https://doi.org/10.48758/ufz.14386> (2023).
165. Droppers, B., Wanders, N. & Bierkens, M. PCR-GLOBWB community reference output - 4dHydro working package 2 <https://doi.org/10.24416/UU01-YA6SFX> (2023).
166. Cortes-Torres, N., de León Pérez, D. & Frances, F. TETIS 4DHydro simulations Po <https://doi.org/10.5281/zenodo.10245905> (2023).
167. Cortes-Torres, N., de León Pérez, D. & Frances, F. TETIS 4DHydro simulations Tugela <https://doi.org/10.5281/zenodo.10246521> (2023).
168. Weerts, A. H. & Imhoff, R. O. 4DHydro Benchmark Dataset wflow\_sbm <https://doi.org/10.4121/6d391c3d-d3d7-4fa2-ae0e-4584776ac3e4.v1> (2023).

## Acknowledgements

The 4DHydro initiative is funded by the European Space Agency (ESA) under contract 4000141141/23/I-EF.

## Author contributions

B.D. and O.R. coordinated the working package; B.D., O.R., L.A., S.A., N.C., D.L. and R.I. formatted and provided the model simulations; B.D. conducted the technical validation; F.F., S.K., R.R. and A.W. coordinated their modeling groups; L.S. coordinated the project. All authors contributed to and reviewed the manuscript.

## Competing interests

The authors declare no competing interests.

## Additional information

**Supplementary information** The online version contains supplementary material available at <https://doi.org/10.1038/s41597-024-03825-9>.

**Correspondence** and requests for materials should be addressed to B.D. or O.R.

**Reprints and permissions information** is available at [www.nature.com/reprints](http://www.nature.com/reprints).

**Publisher's note** Springer Nature remains neutral with regard to jurisdictional claims in published maps and institutional affiliations.



**Open Access** This article is licensed under a Creative Commons Attribution-NonCommercial-NoDerivatives 4.0 International License, which permits any non-commercial use, sharing, distribution and reproduction in any medium or format, as long as you give appropriate credit to the original author(s) and the source, provide a link to the Creative Commons licence, and indicate if you modified the licensed material. You do not have permission under this licence to share adapted material derived from this article or parts of it. The images or other third party material in this article are included in the article's Creative Commons licence, unless indicated otherwise in a credit line to the material. If material is not included in the article's Creative Commons licence and your intended use is not permitted by statutory regulation or exceeds the permitted use, you will need to obtain permission directly from the copyright holder. To view a copy of this licence, visit <http://creativecommons.org/licenses/by-nc-nd/4.0/>.

© The Author(s) 2024